

## Collagen-Derived *N*-Acetylated Proline-Glycine-Proline in Intervertebral Discs Modulates CXCR1/2 Expression and Activation in Cartilage Endplate Stem Cells to Induce Migration and Differentiation Toward a Pro-Inflammatory Phenotype

CHENCHENG FENG, YANG ZHANG, MINGHUI YANG, BO HUANG, YUE ZHOU

**Key Words.** Degenerative disc • *N*-Acetylated proline-glycine-proline • Cartilage endplate stem cell • Migration • Pro-inflammatory phenotype

Department of Orthopedics, Xinqiao Hospital, Third Military Medical University, Chongqing, People's Republic of China

Correspondence: Bo Huang, Ph.D., Xinqiao Main Street 183, Shapingba District, Chongqing, People's Republic of China. Telephone: + 86-02368774328; Fax: + 86-02368774328; e-mail: fmmuhb@126.com; or Yue Zhou, Ph.D., Xinqiao Main Street 183, Shapingba District, Chongqing, People's Republic of China. Telephone: + 86-02368774328; Fax: + 86-02368774328; e-mail: happyzhou@vip.163.com

Received March 18, 2015; accepted for publication July 25, 2015; first published online in STEM CELLS EXPRESS August 25, 2015.

© AlphaMed Press  
1066-5099/2014/\$30.00/0

<http://dx.doi.org/10.1002/stem.2200>

This is an open access article under the terms of the Creative Commons Attribution-NonCommercial-NoDerivs License, which permits use and distribution in any medium, provided the original work is properly cited, the use is non-commercial and no modifications or adaptations are made.

### ABSTRACT

The factors that regulate the migration and differentiation of cartilage endplate stem cells (CESCs) remain unknown. *N*-Acetylated proline-glycine-proline (*N*-Ac-PGP) is a chemokine that is involved in inflammatory diseases. The purpose of this study was to detect *N*-Ac-PGP in degenerative intervertebral discs (IVDs) and to determine its roles in the migration and differentiation of CESCs. Enzyme-linked immunosorbent assay (ELISA) and liquid chromatography-mass spectrometry results indicated that the levels of the proteases that generate *N*-Ac-PGP as well as *N*-Ac-PGP levels themselves increase with the progression of IVD degeneration. Immunohistochemistry and an *N*-Ac-PGP generation assay demonstrated that nucleus pulposus (NP) cells generate *N*-Ac-PGP from collagen. The effects of *N*-Ac-PGP on the migration and differentiation of CESCs were determined using migration assays, RT-PCR, immunoblot analysis, and ELISA. The results showed that the expression of *N*-Ac-PGP receptors (CXCR1 and CXCR2) in CESCs was upregulated by *N*-Ac-PGP. Additionally, *N*-Ac-PGP induced F-actin cytoskeletal rearrangement in CESCs and increased CESC chemotaxis. Furthermore, *N*-Ac-PGP recruited chondrocytes and spindle-shaped cells from the cartilage endplate (CEP) into the NP *in vivo*. These spindle-shaped cells expressed CD105 and Stro-1 (mesenchymal stem cell markers). *N*-Ac-PGP induced the differentiation of CESCs toward a pro-inflammatory phenotype with increased production of inflammatory cytokines rather than toward an NP-like phenotype. Our study indicated that, in the complex microenvironment of a degenerative disc, *N*-Ac-PGP is generated by NP cells and induces the migration of CESCs from the CEP into the NP. *N*-Ac-PGP induces a pro-inflammatory phenotype in CESCs, and these cells promote the inflammatory response in degenerative discs. STEM CELLS 2015;33:3558–3568

### SIGNIFICANCE STATEMENT

In this study, we found that *N*-Ac-PGP generated during intervertebral disc degeneration (IDD) is a factor that induces the migration of Cartilage Endplate Stem Cells (CESCs) from the cartilage endplate into the nucleus pulposus (NP) and CESCs differentiation toward a pro-inflammatory phenotype that elevates the cytokine levels in the microenvironment of degenerative discs. IDD is associated with chronically increased levels of numerous pro-inflammatory cytokines that mediate matrix degradation, immune cell infiltration, and cell senescence in the IVD. Thus, pro-inflammatory CESCs promote the progression of IDD, rather than suppress it. Our study identified a factor that regulates the migration and immune plasticity of CESCs. Furthermore, our study suggests that the suppression of this pro-inflammatory differentiation of CESCs relieves the inflammatory signaling in degenerative discs and contributes to their repair and regeneration.

### INTRODUCTION

Intervertebral disc degeneration (IDD) is a widely recognized contributor to low back pain (LBP) [1, 2]. IDD is a cytokine-mediated patho-

logical process caused by occupational exposures, aging, smoking, infection, trauma, excessive mechanical loading, decreased nutrient supply, and genetic predisposition. IDD is characterized by a loss of disc height and

dehydration of the nucleus pulposus (NP), which can be visualized as a low-intensity signal by T2-weighted MRI, together with structural deficits, inflammation, and herniation of the NP. Prevention or reversal of IDD has been widely accepted as a promising treatment for LBP.

Recently, mesenchymal stem cell (MSC)s have been shown to differentiate into NP-like cells that assist in the regeneration of the intervertebral disc (IVD) [3, 4]. MSC-based therapy has been widely accepted as an advanced biological treatment for IDD. Previously, we demonstrated the presence of resident stem cells, designated cartilage endplate stem cells (CESCs), in the degenerative cartilage endplate (CEP). CESCs share many phenotypical and morphological similarities with bone marrow-MSCs (BM-MSCs), and CESCs exhibit better chondrogenesis and osteogenesis differentiation potentials than BM-MSCs [5, 6]. Thus, CESCs, which are recognized as a type of MSC that resides in the CEP, represent a new strategy for IVD regeneration. Endogenous CESCs are expected to migrate into the NP from the CEP and to differentiate into an NP-like phenotype. However, chemoattractants that recruit CESCs have not been investigated in the IVD. Moreover, the complex microenvironment of a degenerative disc is characterized by hypoxia, low nutrition, and numerous cytokines [7]. Whether CESCs differentiate toward an NP-like phenotype in this harsh microenvironment remains unknown. Notably, MSCs have been shown to possess immune plasticity. Activation of Toll-like receptors (TLRs) on MSCs endows these cells with a pro-inflammatory phenotype characterized by the increased production of various cytokines, including IL-1 $\beta$ , IL-6, IL-8, and CCL5 [8]. These pro-inflammatory mediators have been shown to mediate the IDD process [9]. Thus, CESCs likely acquire a pro-inflammatory phenotype to accelerate the progression of IDD.

*N*-acetylated proline-glycine-proline (*N*-Ac-PGP) is a collagen-derived tripeptide that is generated via a multistep proteolytic pathway involving matrix metalloprotease (MMP) 8, MMP9, and prolyl endopeptidase (PE) [10]. *N*-Ac-PGP is a potent chemokine for neutrophils via CXC receptor (CXCR) 1 and CXCR2 [11] and plays an important role in neutrophilic inflammatory diseases, such as chronic obstructive pulmonary disease (COPD) and inflammatory bowel diseases (IBDs) [12, 13]. During the process of IDD, increased MMP production and enhanced collagen degradation have been extensively investigated [14]. However, the presence of *N*-Ac-PGP in degenerative discs and the effects of *N*-Ac-PGP on the migration and differentiation of CESCs remain unknown.

This study aimed to measure the levels of MMP8, MMP9, PE, and *N*-Ac-PGP in IVD specimens. We identified the cells that generate *N*-Ac-PGP in IVD. To determine whether *N*-Ac-PGP is a potent chemokine in the IVD, we performed *in vitro* and *in vivo* chemotaxis assays. We also investigated the effects of *N*-Ac-PGP on CESC differentiation. We hypothesized that disc cells generate *N*-Ac-PGP from collagen through the proteolytic pathway during the progression of IDD. *N*-Ac-PGP recruits CESCs from the CEP into the NP via CXCR1/2. Moreover, *N*-Ac-PGP binding to CXCR1/2 suppresses the differentiation of CESCs toward an NP-like phenotype, whereas CESCs acquire a pro-inflammatory phenotype with *N*-Ac-PGP stimulation. Our results indicate that, in the complex microenvironment of degenerative discs, CESCs may exert negative roles

rather than positive roles in the structural and functional maintenance of the IVD. Additionally, the inhibition of *N*-Ac-PGP generation promotes the positive roles of *N*-Ac-PGP in IVD repair and regeneration.

## MATERIALS AND METHODS

### Reagents

*N*-Ac-PGP and human collagen type II were purchased from Sigma-Aldrich (St. Louis, Missouri, <http://www.sigmaaldrich.com/>). A CXCR1 antagonist (Repertaxin) was provided by MedChemexpress (Princeton, New Jersey, <http://www.medchemexpress.com/>). A CXCR2 antagonist (SB225002) was purchased from Abcam (Cambridge, Massachusetts, <http://www.abcam.com/>). Goat antibodies against GAPDH, MMP8, MMP9, and PE as well as mouse antibodies against CXCR1, CXCR2, Stro-1, MT-MMP1, CD105, SOX-9, Aggrecan, and collagen type II were purchased from Santa Cruz Biotechnology (Santa Cruz, Dallas, Texas, <http://www.scbt.com/>). Relevant horse reddish peroxidase (HRP)-conjugated secondary antibodies and FITC-conjugated secondary antibodies were purchased from ZSGB-BIO (Beijing, People's Republic of China, <http://www.zsbio.com/>).

### Human IVD Specimens

Lumbar disc specimens were obtained from patients undergoing posterior discectomy and a fusion procedure for IDD at Xinqiao Hospital. The specimens were divided into two groups according to their Pfirrmann grade [15]. The severe degeneration group comprised tissues from 30 patients (Pfirrmann grade  $\geq$  IV,  $n = 30$ ), and the mild degeneration group comprised tissues from 25 patients (Pfirrmann grade  $\leq$  III,  $n = 25$ ). For grades  $\leq$  III, the T2-weighted signal intensity of the NP is hyperintense white or gray, but for grades  $\geq$  IV, it is hypointense dark or black [15]. The signal loss of the NP is directly related to the biochemical, histological, and progressive degenerative changes of the IVD [16–18]. Moreover, the distinction between NP and annulus fibrosus (AF) is distinguishable in discs with grades  $\leq$  III, but it is lost in discs with grades  $\geq$  IV. With more severe disc degeneration, there is no distinction between the NP and AF [15]. These facts suggest that discs with grades  $\geq$  IV present more severe degenerative features than discs with grades  $\leq$  III. Thus, the breakpoint was set at grade III or less and grade IV or more to populate the two groups. The NP and CEP tissues were separated by three surgeons via a previously described protocol [19]. All protocols for obtaining human IVD samples were approved by the Ethical Committee of Xinqiao Hospital and were in accordance with the Declaration of Helsinki. Detailed information regarding the patients and samples is shown in Table 1. There were no significant differences in mean age and gender between the two groups.

### Preparation of NP Tissues for Enzyme-Linked Immunosorbent Assay

NP tissues (mild degeneration group:  $n = 7$ ; severe degeneration group:  $n = 8$ ) were weighed and ground in liquid nitrogen. The obtained tissue powders were dissolved in RIPA lysis buffer containing phenylmethanesulfonyl fluoride (PMSF) (100 mg tissue/ml; Beyotime, Shanghai, People's Republic of

**Table 1.** Demographic information of donors and the usage of disc samples

No. of donors	25	30
No. of total samples	25	30
Age, mean $\pm$ SD years	57 $\pm$ 3	47 $\pm$ 4
Age range, years	30-75	41-77
Men, %	64	45
No. of samples (Pfirsman score=I)	5	0
No. of samples (Pfirsman score=II)	9	0
No. of samples (Pfirsman score=III)	11	0
No. of samples (Pfirsman score=IV)	0	18
No. of samples (Pfirsman score=V)	0	12
No. of samples for ELISA	7	8
No. of samples for N-Ac-PGPassay	11	11
No. of samples for ex vivo assay	7	11

Abbreviation: N-Ac-PGP, N-acetylated proline-glycine-proline.

China, <http://www.beyotime.com/>) and then centrifuged for 10 minutes at 15,000 rpm at 4°C. The supernatants were transferred to clean tubes.

### Preparation of NP Tissues for N-Ac-PGP Measurement

NP tissues (mild degeneration group:  $n_I = 2$ ,  $n_{II} = 4$ ,  $n_{III} = 5$ ; severe degeneration group:  $n_{IV} = 6$ ,  $n_V = 5$ ) were weighed and homogenized in ultrapure water (100 mg tissue/ml) using a glass homogenizer. The homogenates were centrifuged for 15 minutes at 12,000 rpm at 4°C and then loaded onto Oasis HLB columns (1 ml, Waters Corporation, Milford, Massachusetts, <http://www.waters.com/>). One hundred microliters of 10% methanol in water was used to elute the analytes.

### Cell Culture and Ex Vivo N-Ac-PGP Generation Assay

NP cells and C ESCs were isolated from specimens and incubated in Dulbecco's modified Eagle's medium (DMEM)/F-12 containing 10% fetal calf serum and 1% penicillin-streptomycin (Invitrogen Gibco, Waltham, Massachusetts, <https://www.thermofisher.com/>) as previously described [5, 6]. For the ex vivo N-Ac-PGP generation assay, 90  $\mu$ l of conditioned media from NP cells (mild degeneration group:  $n = 7$ ; severe degeneration group:  $n = 11$ ) was harvested and incubated with 10  $\mu$ l of a 1 mg/ml collagen type II solution for 24 hours at 37°C. The collagen solution was predialyzed to remove N-Ac-PGP. The conditioned media were also harvested for enzyme-linked immunosorbent assay (ELISA). C ESCs were identified by flow cytometry analysis as previously described (data not shown) [5, 20]. The cells were used in experiments at the second passage.

### Electrospray Ionization Liquid Chromatography-Mass Spectrometry to Measure N-Ac-PGP

N-Ac-PGP levels in NP tissues and in the ex vivo N-Ac-PGP generation assay were measured as described previously [21]. The samples were analyzed using an Agilent 1290 Infinity Quaternary LC System (Agilent Technologies, Santa Clara, California, <http://www.agilent.com/>) on Eclipse Plus C18 columns (150 mm  $\times$  2.1 mm, 3.5  $\mu$ m; Agilent Technologies). Positive electrospray mass transitions were monitored at 312 > 140 and 312 > 112 for N-Ac-PGP.

### In Vitro Chemotaxis Assay

The chemotactic response of C ESCs to N-Ac-PGP was investigated using a transwell migration assay (8- $\mu$ m pore mem-

brane, Millipore, Darmstadt, Germany, <http://www.emdmillipore.com/>). C ESCs were starved in serum-free DMEM/F-12 for 24 hours and then transferred to the upper chambers ( $3 \times 10^5$  cells) in 100  $\mu$ l of serum-free DMEM/F-12. Different concentrations of N-Ac-PGP (0, 1, 10, 100, and 1,000  $\mu$ g/ml) in 500  $\mu$ l of DMEM/F-12 were added to the lower chambers. For the inhibition assays, CXCR1/2 antagonists (10  $\mu$ g/ml) were added to the upper wells. After a 10-hour incubation at 37°C and 5% CO<sub>2</sub>, the membranes were fixed in 4% paraformaldehyde and stained with 1% crystal violet. The numbers of migrated cells in nine random fields were counted using a microscope ( $\times 200$ ).

### F-Actin Staining

F-actin was detected using a CytoPainter F-actin staining kit (ab112127, Abcam). Briefly, C ESCs treated with N-Ac-PGP (100  $\mu$ g/ml) for 72 hours were fixed with 4% paraformaldehyde for 20 minutes and then incubated with 100  $\mu$ l of red fluorescent phalloidin conjugate working solution (this working solution was prepared according to the protocol provided by the manufacturer) at room temperature for 60 minutes. The cells were washed three times in phosphate buffered saline (PBS) and imaged using the Texas Red channel ( $E_x/E_m = 594/610$  nm). CXCR1/2 antagonists (10  $\mu$ g/ml) were used for the inhibition assays, and C ESCs without N-Ac-PGP treatment served as the controls. The fluorescence intensities were calculated using ImageJ.

### In Vivo Chemotaxis Assay

Eighteen 2-month-old New Zealand white rabbits were used in this study. The rabbits were randomized into six groups. Under pentobarbital anesthesia, intradiscal delivery of N-Ac-PGP (50  $\mu$ l, 100  $\mu$ g/ml) or PBS into the lumbar disc was performed. For the inhibition assays, CXCR1/2 antagonists (50  $\mu$ l, 10  $\mu$ g/ml) were delivered into lumbar discs 20 minutes before N-Ac-PGP treatment. Rabbits were monitored until sacrifice on day 7. Lumbar discs were collected to determine the chemotactic effects of N-Ac-PGP on IVD cells by histological analysis. Animal studies were approved by the Ethical Committee of Xinqiao Hospital.

### N-Ac-PGP-Induced Differentiation Assay

C ESCs were treated with N-Ac-PGP (100  $\mu$ g/ml) for 72 hours. Total RNA was isolated from C ESCs according to the TRIzol RNA isolation protocol (Takara Bio, Shiga, Japan, <http://www.clontech.com/>). Conditioned media were harvested for ELISA. Total protein extracts from C ESCs were obtained using RIPA lysis buffer containing PMSF and then were analyzed by immunoblotting. CXCR1/2 antagonists (10  $\mu$ g/ml) were used for the inhibition assays. C ESCs that were not treated with N-Ac-PGP served as the controls.

### Histological Analysis

Disc specimens were fixed, embedded in paraffin, and sectioned sagittally at a thickness of 5  $\mu$ m. For in vivo chemotaxis assays, sections were stained with hematoxylin and eosin (H&E). For immunohistochemistry assays, paraffin sections were deparaffinized and rehydrated. After blocking endogenous peroxidase activity and performing heat-mediated antigen retrieval, the sections were incubated with primary antibodies against MMP8 (1:100 dilution), MMP9 (1:50

dilution), PE (1:200 dilution), MT-MMP1 (1:100 dilution), and mesenchymal stem cell markers (CD105 and Stro-1, 1:100 dilution) overnight at 4 °C. The sections were then incubated with HRP-conjugated secondary antibodies at room temperature. The immunoreactive products were detected with diaminobenzidine (Sigma-Aldrich). The sections were counterstained with hematoxylin. Slides that were not incubated with primary antibodies served as the negative controls. Photomicrographs were obtained with an Olympus BX60 microscope (Olympus, Tokyo, Japan, <http://cn.olympus.com/>).

### Immunofluorescence Assay

Cells plated in culture dishes were fixed with 4% paraformaldehyde, permeabilized with 0.2% Triton X-100 in PBS, and blocked with PBS containing 1% bovine serum albumin; the cells were subsequently incubated with primary antibodies against MMP8 (1:100 dilution), MMP9 (1:50 dilution), PE (1:200 dilution), CXCR1 (1:200 dilution), and CXCR2 (1:50 dilution) overnight at 4 °C. After PBS washes, cells were incubated with FITC-conjugated secondary antibodies in the dark and then stained with 4,6-diamidino-2-phenylindole (0.1 mg/ml, Sigma-Aldrich). Cells that were not incubated with primary antibodies served as the negative controls. Images were obtained using a confocal laser scanning microscope.

### ELISA

The concentrations of cytokines (CCL2, IL-1 $\beta$ , TNF- $\alpha$ , TGF- $\beta$ , MMP8, MMP9, and PE) were measured using ELISA kits (Westang Biotechnology, Shanghai, People's Republic of China, <http://www.westang.com/>). Samples were diluted based on the sensitivities of the kits. The protocols were provided by the manufacturer. The optical density was measured at 450 nm using a spectrophotometer [Varioskan Flash, Thermo Scientific (Applied Biosystems, Life Technologies), Waltham, Massachusetts, <https://www.thermofisher.com/>].

### Real-Time RT-PCR

Total RNA (1  $\mu$ g) was used to synthesize cDNA using a PrimeScript RT Reagent Kit (Takara Bio) according to the manufacturer's instructions. Real-time RT-PCR assays were performed in duplicate on a StepOnePlus Real-Time PCR system (Applied Biosystems) with SYBR Premix Ex Taq II (Takara Bio). GAPDH was used as the internal reference gene. A 20- $\mu$ l reaction volume was used. The reactions were run under the following conditions: 95 °C for 30 seconds followed by 40 cycles of 95 °C for 5 seconds and 60 °C for 34 seconds. The relative gene expression was calculated using the  $\Delta\Delta C_t$  method and was normalized to the gene expression of the control.

### Immunoblot Analysis

Protein samples were separated on 10% (wt/vol) sodium dodecyl sulfate (SDS) gels and transferred onto polyvinylidene fluoride (PVDF) membranes (Millipore). The membranes were blocked with 5% milk proteins in Tris-buffered saline with Tween (TBST) for 1 hour at 37 °C and then incubated with primary antibodies (anti-GAPDH, 1:1,000 dilution; anti-MMP8, 1:700 dilution; anti-MMP9, 1:700 dilution; anti-PE, 1:700 dilution; anti-CXCR1, 1:700 dilution; anti-CXCR2, 1:700 dilution; anti-SOX-9, 1:1,000 dilution; anti-aggreccan, 1:700 dilution; and anti-collagen type II, 1:700 dilution) overnight at 4 °C. The membranes were then incubated with HRP-conjugated

secondary antibodies for 1 hour at 37 °C. Immunolabeling was detected using electrochemiluminescence (ECL) reagent (Thermo Scientific).

### Statistical Analysis

All measurements were performed in triplicate, and the data are presented as the mean  $\pm$  SEM. For comparisons between two groups, a two-tailed Student's *t* test was used. For comparisons among three or more groups, one-way ANOVA, Dunnett's multiple comparisons, and least-significant difference (LSD) multiple comparisons were used. The data obtained from the real-time RT-PCR assays were analyzed using Kruskal-Wallis nonparametric analysis and Mann-Whitney *U* post hoc tests as described elsewhere [22]. The data were analyzed using GraphPad Prism 5 or SPSS version 20.0. *p* < .05 was considered statistically significant.

## RESULTS

### Protease Assay in NP Tissues

MMP8, MMP9, and PE were detected in NP tissues. The levels of MMP8 and MMP9 were significantly higher in NP tissues from the severe degeneration group than from the mild degeneration group (Fig. 1A). The levels of PE were slightly higher in NP tissues from the mild degeneration group, but the difference between the two groups was not significant (Fig. 1A).

### Measurement of *N*-Ac-PGP in NP Tissues

Figure 1B illustrates a typical multiple reaction monitoring (MRM) chromatogram of *N*-Ac-PGP (*m/z* 312/112) in NP tissues, which was consistent with the MRM chromatogram of standard *N*-Ac-PGP (*m/z* 312/112) (Fig. 1B). The *N*-Ac-PGP levels were significantly higher in NP tissues from the severe degeneration group than from the mild degeneration group (Fig. 1C). *N*-Ac-PGP levels increased as Pfirrmann scores of NP tissues increased (Fig. 1D), and *N*-Ac-PGP levels were positively correlated with Pfirrmann scores (Spearman's *r* = .846, *p* < .05).

### NP Cells Generated *N*-Ac-PGP

MMP8, MMP9, and PE were expressed in NP cells in vivo and in vitro (Fig. 2A, 2B). Cultured NP cells expressed these proteases in the cytoplasm (Fig. 2B). The levels of MMP8 and MMP9 were significantly higher in the conditioned media from NP cells in the severe degeneration group than from NP cells in the mild degeneration group. The levels of PE were not significantly different between the two groups (Supporting Information Fig. S1). Moreover, conditioned media from the severe degeneration group generated more *N*-Ac-PGP from collagen than from the mild degeneration group (Fig. 2D; a typical MRM chromatogram is shown in Fig. 2C).

### *N*-Ac-PGP Was a Chemokine for CESC

CXCR1 and CXCR2 were expressed in the cell membrane and cytoplasm of CESC (Fig. 3A). *N*-Ac-PGP treatment upregulated the expression of CXCR1/2 in CESC (Fig. 3B, 3C). CESC spontaneously migrated across the transwell membrane. *N*-Ac-PGP at concentrations of 100  $\mu$ g/ml and 1,000  $\mu$ g/ml significantly induced the migration of CESC, and *N*-Ac-PGP at 1,000  $\mu$ g/ml recruited more CESC than *N*-Ac-PGP at 100  $\mu$ g/ml. The number of migrated cells was also increased by *N*-Ac-PGP at

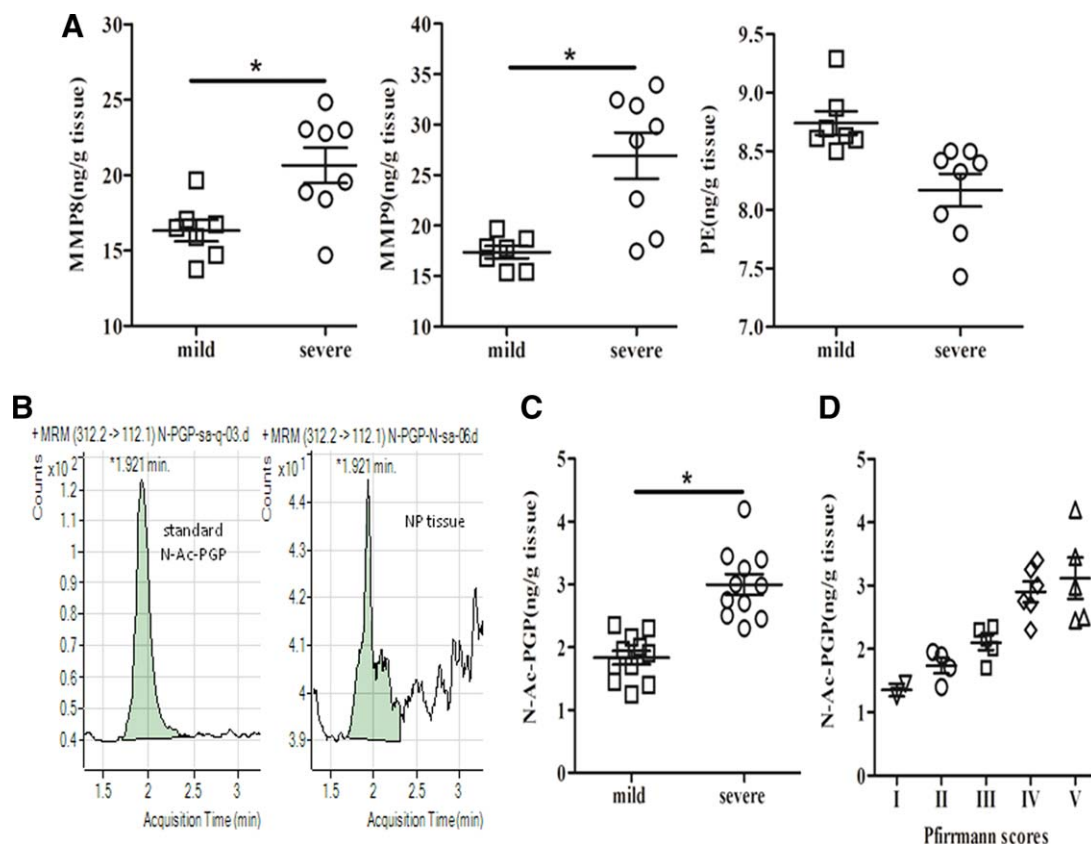


**Figure 1.** Protease and *N*-Ac-PGP levels in NP tissues. **(A):** The expression of MMP8, MMP9, and PE in homogenates of NP tissues from patients with mild disc degeneration (mild,  $n = 7$ ) and from patients with severe disc degeneration (severe,  $n = 8$ ). **(B):** Typical MRM chromatograms of the *N*-Ac-PGP standard ( $m/z$  312/112) and *N*-Ac-PGP ( $m/z$  312/112) in NP tissue homogenates. A single peak at the same acquisition time as standard *N*-Ac-PGP was observed in NP tissue homogenates. **(C):** *N*-Ac-PGP levels in NP tissue homogenates from patients with mild disc degeneration (mild,  $n = 11$ ) and severe disc degeneration (severe,  $n = 11$ ). **(D):** *N*-Ac-PGP levels increased with Pfirrmann scores of NP tissues increased ( $n_I = 2$ ,  $n_{II} = 4$ ,  $n_{III} = 5$ ,  $n_{IV} = 6$ , and  $n_V = 5$ ). Individual results are shown, horizontal lines represent the mean, and error bars represent the SEM. \*,  $p < .05$ . Abbreviations: MMP8, matrix metalloproteinase 8; MRM, multiple reaction monitoring; *N*-Ac-PGP, *N*-acetylated proline-glycine-proline; NP, nucleus pulposus; PE, prollyl endopeptidase.

concentrations of 1  $\mu\text{g/ml}$  and 10  $\mu\text{g/ml}$ , but there was no statistical difference (Fig. 3D). Antagonizing CXCR1 and CXCR2 alone or simultaneously significantly suppressed the CESC migration induced by *N*-Ac-PGP (Fig. 3E).

### F-Actin Staining

*N*-Ac-PGP enhanced F-actin cytoskeletal remodeling and lamellipodia formation in C ESCs. The fluorescence intensity of F-actin was the highest in C ESCs treated with *N*-Ac-PGP. Antagonizing CXCR1 or CXCR2 individually inhibited the cytoskeletal rearrangements induced by *N*-Ac-PGP, and antagonizing both receptors had a synergistic effect (Fig. 3F).

### *N*-Ac-PGP Induced the Migration of Cells Residing in the Rabbit CEP

An H&E-stained sagittal section of a normal rabbit lumbar disc is shown in Figure 4A. The cells residing in the CEP exhibited two different cellular morphologies indicative of chondrocytes and spindle-shaped cells (Fig. 4A). Intradiscal delivery of *N*-Ac-PGP induced the migration of chondrocytes and spindle-shaped cells from the CEP into the NP (Fig. 4B); intradiscal delivery of PBS had no effect (Fig. 4C). Antagonizing CXCR1 or CXCR2 incompletely suppressed the migration induced by *N*-Ac-PGP, whereas antagonizing both receptors completely

suppressed the migration induced by *N*-Ac-PGP (Fig. 4C). The migratory chondrocytes and spindle-shaped cells expressed MT-MMP1. CD105 and Stro-1 were expressed in the migratory spindle-shaped cells, and the migratory chondrocytes expressed CD105 (Fig. 4D).

### *N*-Ac-PGP Suppressed the Differentiation of C ESCs Toward an NP-Like Phenotype

*N*-Ac-PGP downregulated the expression of aggrecan, collagen type II, and SOX-9 in C ESCs. The downregulated expression of aggrecan was suppressed by antagonizing CXCR1 and 2 simultaneously. The downregulated expression of SOX-9 was inhibited by antagonizing CXCR2 alone or antagonizing both receptors simultaneously. Antagonizing CXCR1/2 individually reversed the downregulated expression of collagen type II, and antagonizing both receptors synergistically inhibited this downregulated expression (Fig. 5A). These results were consistent with the results of the immunoblot analysis (Fig. 5B).

### *N*-Ac-PGP Induced the Differentiation of C ESCs Toward a Pro-Inflammatory Phenotype with Increased Production of Inflammatory Mediators

IL-1 $\beta$  and TNF- $\alpha$  mediate the pathogenesis of IDD [23–25]. C ESCs treated with *N*-Ac-PGP secreted more TNF- $\alpha$  and IL-1 $\beta$

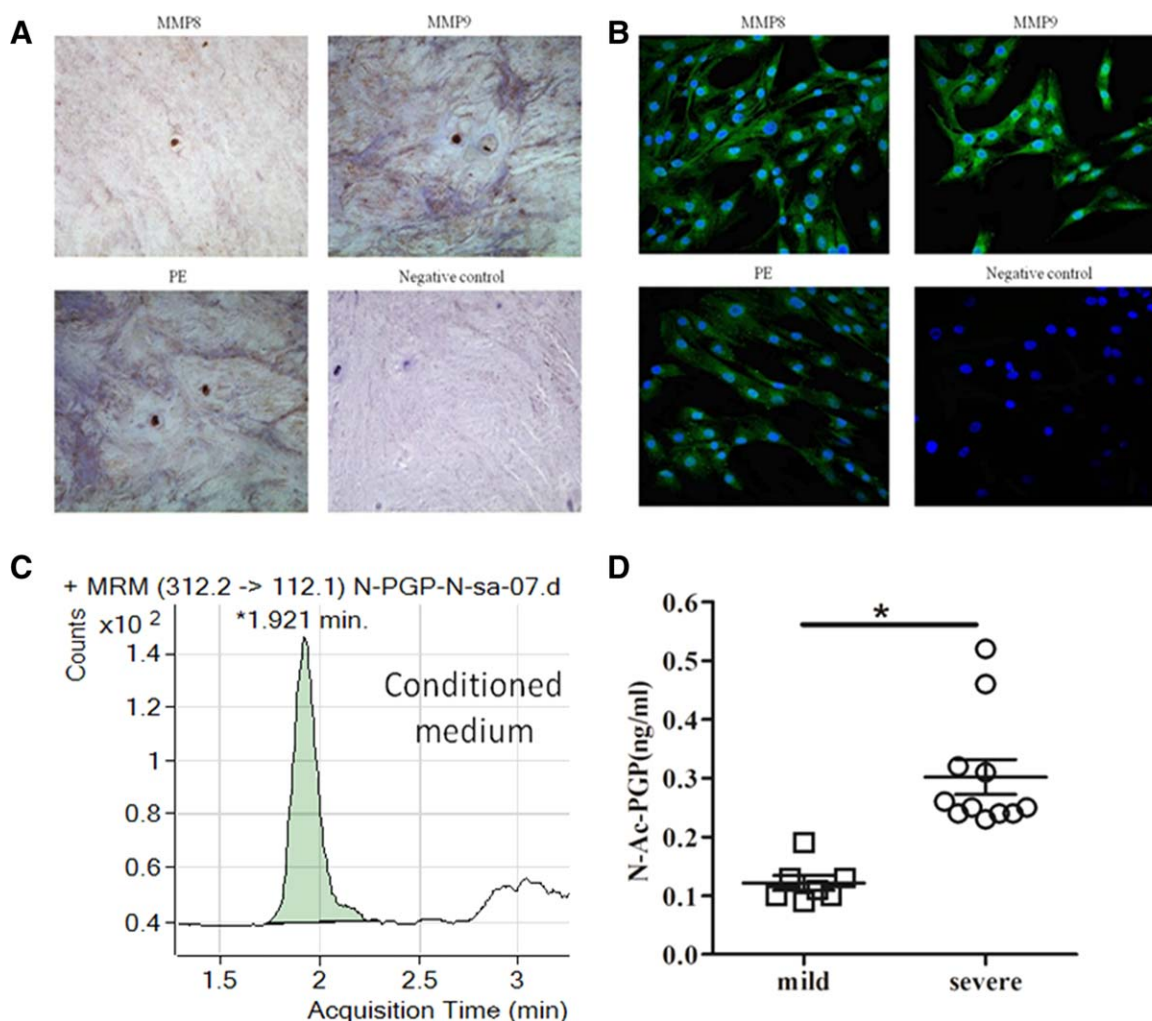


**Figure 2.** Protease expression and *N*-Ac-PGP generation by NP cells from patients with intervertebral disc degeneration. **(A):** Immunohistochemical staining for MMP8, MMP9, and PE as well as a negative control in NP tissues. NP cells expressed MMP8, MMP9, and PE *in vivo*. Original magnification,  $\times 400$ . **(B):** Immunofluorescence staining of MMP8, MMP9, and PE expression in cultured NP cells. Fluorescence corresponding to MMP8, MMP9, and PE was detected in the cytoplasm of NP cells. Original magnification,  $\times 100$ . **(C):** Typical MRM chromatograms of *N*-Ac-PGP ( $m/z$  312/112) generated from collagen type II with conditioned media from NP cells. A single peak at the same acquisition time as standard *N*-Ac-PGP (Fig. 1B) was observed. **(D):** *N*-Ac-PGP generated from collagen type II with conditioned media from NP cells from the mild degeneration group (mild,  $n = 7$ ) and from the severe degeneration group (severe,  $n = 11$ ). Individual results are shown, horizontal lines represent the mean, and error bars represent the SEM. \*,  $p < .05$ . Abbreviations: MMP8, matrix metalloproteinase 8; MRM, multiple reaction monitoring; *N*-Ac-PGP, *N*-acetylated proline-glycine-proline; PE, prolyl endopeptidase.

compared with controls. Antagonizing CXCR1 alone or antagonizing CXCR1 and CXCR2 simultaneously suppressed the increased secretion of TNF- $\alpha$ . CXCR1/2 antagonists suppressed the increased secretion of IL-1 $\beta$  (Fig. 5C). The *N*-Ac-PGP-mediated upregulated expression of TNF- $\alpha$  and IL-1 $\beta$  was inhibited by CXCR1/2 antagonists (Fig. 5D).

Various chemotactic factors have been shown to promote immune cell infiltration in degenerative discs [26, 27]. *N*-Ac-PGP increased the secretion of CCL2 by C ESCs; this increase was suppressed by CXCR1/2 antagonists (Fig. 5C). The expression of CCL2 and CCL5 in C ESCs was upregulated by *N*-Ac-PGP, and this upregulation was inhibited by CXCR1/2 antagonists (Fig. 5D).

Excessive proteases cause pathological degradation of extracellular matrix (ECM) in the degenerative IVD [14]. *N*-Ac-PGP treatment significantly upregulated the expression of MMP8 in C ESCs. CXCR1/2 antagonists repressed the upregulation

of MMP8 expression (Fig. 5D). *N*-Ac-PGP also increased the secretion of MMP8 by C ESCs, which was significantly repressed by the CXCR1 antagonist (Fig. 5C). Meanwhile, *N*-Ac-PGP appeared to slightly upregulate the expression of MMP9 in C ESCs (Fig. 5D), but there was no statistical difference (Fig. 3D).

IFN- $\gamma$  and IL-17 synergistically amplify inflammatory signaling in degenerative discs [28]. We observed the upregulated expression of IFN- $\gamma$  in C ESCs in response to *N*-Ac-PGP treatment; this effect was suppressed by CXCR1/2 antagonists (Fig. 5D).

TGF- $\beta$  is a growth factor that retards the progression of IDD [29]. *N*-Ac-PGP decreased the secretion of TGF- $\beta$  by C ESCs, but this decrease was not repressed by CXCR1/2 antagonists (Fig. 5C). The expression of TGF- $\beta$  in C ESCs exhibited a similar trend (Fig. 5D), indicating that *N*-Ac-PGP binds to receptors other than CXCR1/2 to inhibit the expression and secretion of TGF- $\beta$ .

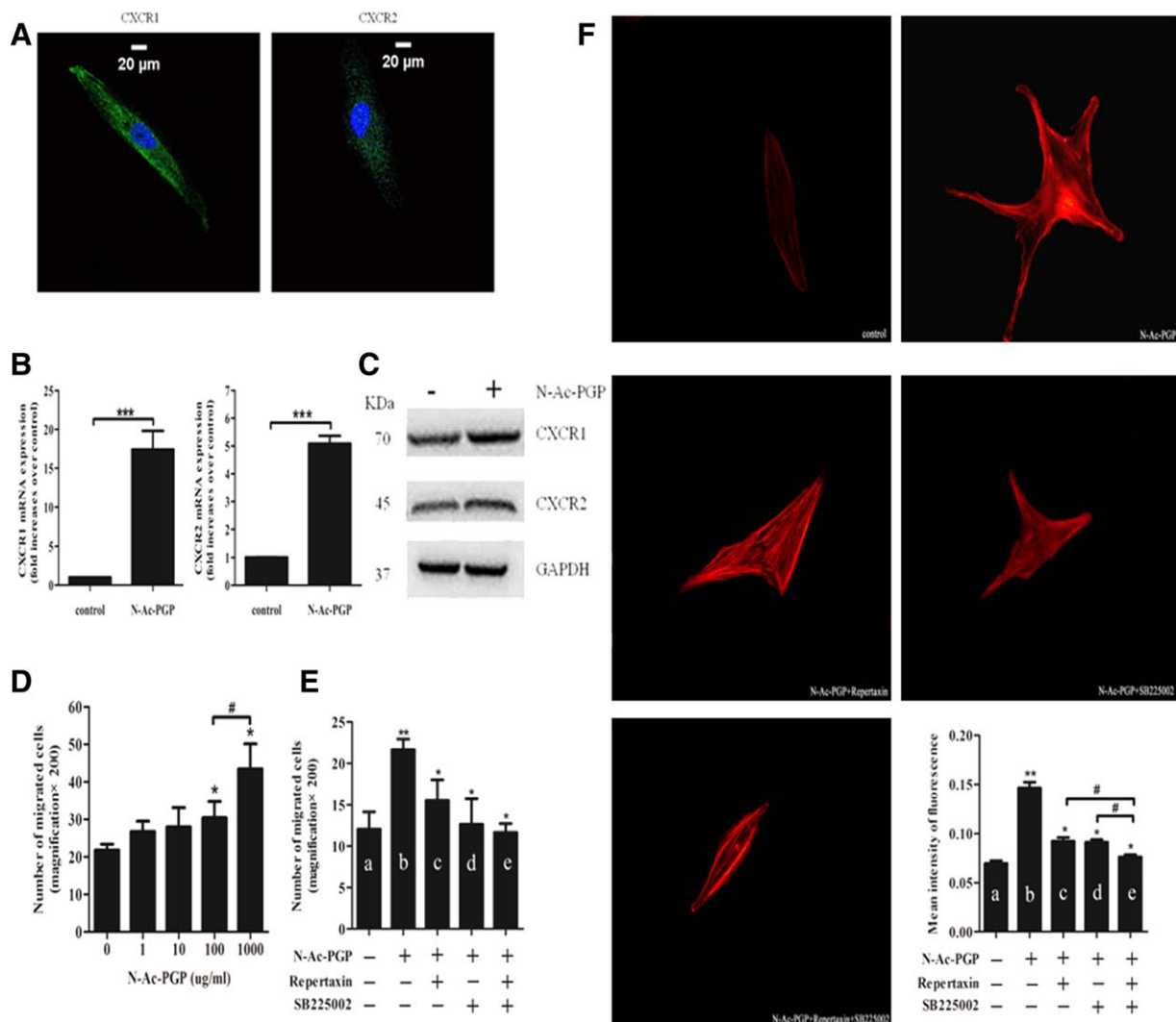


**Figure 3.** In vitro chemotaxis assay. **(A):** Immunofluorescence staining of CXCR1 and CXCR2 in cultured cartilage endplate stem cells (CESCs). Fluorescence was detected in the cytoplasm and cell membrane. Scale bars = 20  $\mu\text{m}$ . **(B):** Real-time RT-PCR analysis of CXCR1 and CXCR2 expression in CESCs. *N*-Ac-PGP upregulated the mRNA expression of CXCR1 and CXCR2 in CESCs. \*\*\*,  $p < .001$ . **(C):** Immunoblot analysis. *N*-Ac-PGP upregulated the expression of CXCR1 and CXCR2 in CESCs. **(D):** Transwell chemotaxis assay. *N*-Ac-PGP at concentrations of 100  $\mu\text{g}/\text{ml}$  and 1,000  $\mu\text{g}/\text{ml}$  significantly induced the migration of CESCs. *N*-Ac-PGP at 1,000  $\mu\text{g}/\text{ml}$  recruited more CESCs than *N*-Ac-PGP at 100  $\mu\text{g}/\text{ml}$ . \*,  $p < .05$  compared to the control group; #,  $p < .05$ . **(E):** Antagonizing CXCR1 and CXCR2 alone or simultaneously inhibited the *N*-Ac-PGP-dependent induction of CESC migration. \*\*,  $p < .05$  compared to a; \*,  $p < .05$  compared to b. **(F):** F-actin staining of the cytoskeleton and lamellipodia in CESCs. *N*-Ac-PGP enhanced the remodeling of F-actin and the formation of lamellipodia in CESCs, and antagonizing CXCR1/2 suppressed the *N*-Ac-PGP-dependent F-actin rearrangement and lamellipodia formation. Fluorescence intensity is presented in the histogram. \*\*,  $p < .05$  compared to a; \*,  $p < .05$  compared to b; #,  $p < .05$ . The data are presented as the mean  $\pm$  SEM. Abbreviation: *N*-Ac-PGP, *N*-acetylated proline-glycine-proline.

## DISCUSSION

In this study, we demonstrated the presence of MMP8, MMP9, and PE in IVD. The levels of *N*-Ac-PGP in NP tissues increased with IDD progression, suggesting a potential role for endogenous *N*-Ac-PGP in the pathogenesis of IDD. We verified that NP cells express MMP8, MMP9, and PE and generate *N*-Ac-PGP from collagen. We observed that CESCs express CXCR1 and CXCR2 and elevate the expression of both receptors in response to *N*-Ac-PGP. We also observed that *N*-Ac-PGP promotes the migration of CESCs in a dose-dependent manner via CXCR1/2. *N*-Ac-PGP enhanced the formation of F-actin and lamellipodia in CESCs. Intradiscal delivery of *N*-Ac-PGP in a

rabbit lumbar disc model induced the migration of chondrocytes and spindle-shaped cells from the CEP into the NP. These migratory spindle-shaped cells expressed Stro-1 and CD105. Finally, we found that the binding of *N*-Ac-PGP to CXCR1/2 induced the differentiation of CESCs toward a pro-inflammatory phenotype rather than an NP-like phenotype.

MMP8 is a type of collagenase that acts on fibrillar collagen. MMP9 is a type of gelatinase that digests denatured collagen [27]. Both proteases are major mediators of collagen degradation. The levels of both proteases increased as IDD progressed, suggesting enhanced matrix degradation in degenerative discs. PE, a member of the serine protease family, has been shown to have a central role in pulmonary neutrophilic

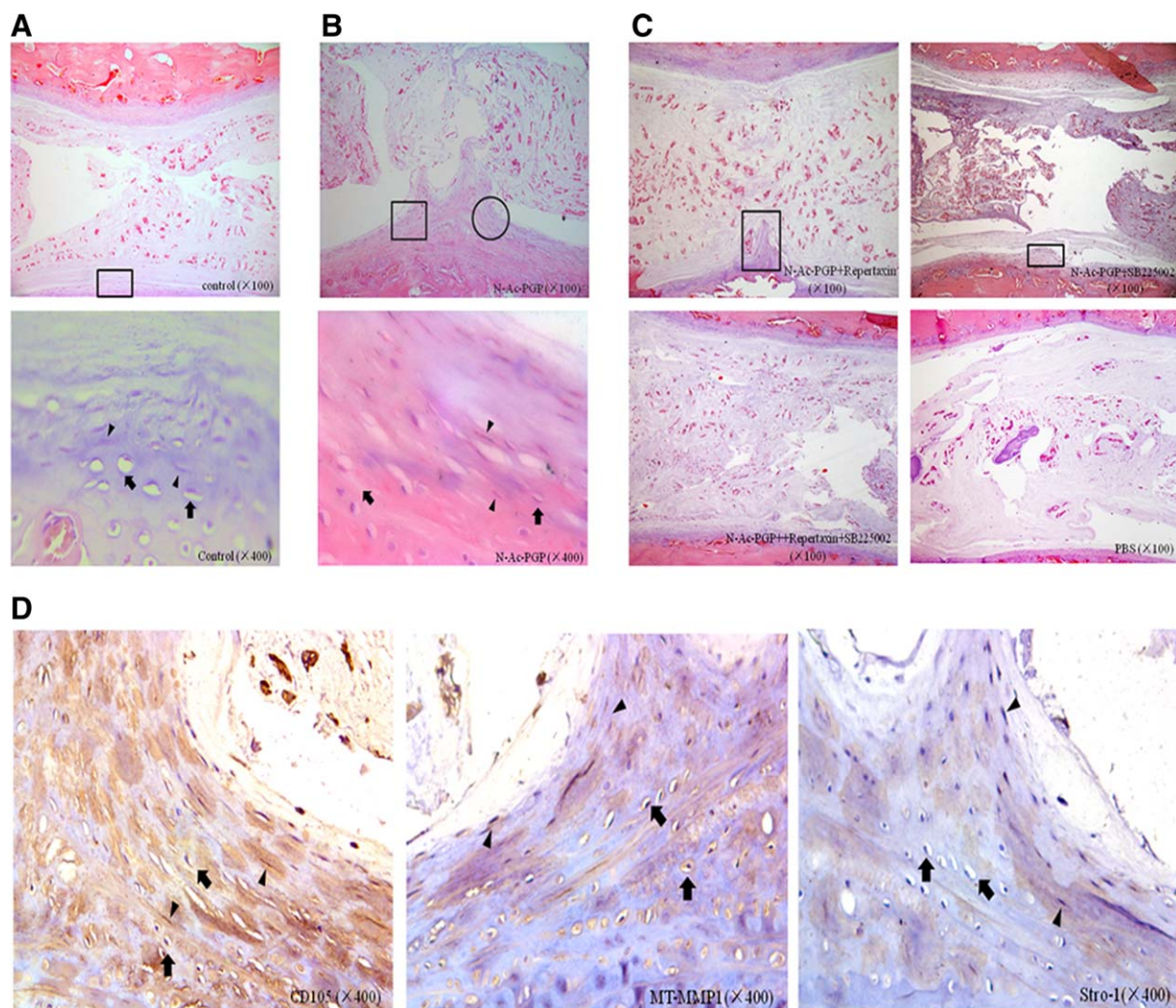


**Figure 4.** Chemotaxis assay in a rabbit lumbar disc model. **(A):** Hematoxylin-eosin (H&E)-stained sagittal sections of a 2-month-old rabbit normal lumbar intervertebral disc. The upper panel shows the cartilage endplate (CEP); a higher magnification view is presented in the boxed area in the upper panel. The CEP contains cells with two different morphologies: chondrocytes (arrows) and spindle-shaped cells (arrowheads). **(B):** H&E-stained sagittal section on day 7 after intradiscal delivery of *N*-Ac-PGP into the lumbar disc. *N*-Ac-PGP induced the invasion of fibrocartilaginous fibers from the caudal CEP into the notochordal nucleus pulposus. The lower panel shows a higher magnification view of the circled area in the upper panel. The fibrocartilaginous fibers are formed by spindle-shaped cells (arrowheads) and chondrocytes (arrows) in the CEP. **(C):** H&E-stained sagittal sections from the inhibition assays. Intradiscal delivery of the CXCR1 or CXCR2 antagonist 20 minutes before *N*-Ac-PGP delivery incompletely repressed the invasion of fibrocartilaginous fibers from the caudal CEP, whereas simultaneously antagonizing both receptors completely suppressed the invasion. Intradiscal delivery of PBS did not induce the invasion of fibrocartilaginous fibers. **(D):** Immunohistochemical staining of MT-MMP1, CD105, and Stro-1 in the boxed and circle areas in Figure 2B. The migratory spindle-shaped cells (arrowheads) expressed MT-MMP1, CD105, and Stro-1, and the migratory chondrocytes (arrows) expressed MT-MMP1 and CD105. Abbreviation: *N*-Ac-PGP, *N*-acetylated proline-glycine-proline.

inflammation and a unique role in the generation of *N*-Ac-PGP [10]. However, PE levels did not increase as the degree of IDD increased, suggesting that MMP8 and MMP9 are the limiting steps in *N*-Ac-PGP generation.

The roles of *N*-Ac-PGP in COPD, cystic fibrosis (CF), and IBD have been investigated [12, 13, 30]. To the best of our knowledge, this is the first study that measured the levels of *N*-Ac-PGP in NP tissues. Previous studies have demonstrated elevated levels of chemoattractants in degenerative discs [26, 27, 31, 32], including CCL2, CCL3, CCL4, IL-8, and CXCL10. These chemoattractants promote the infiltration of macrophages, neutrophils, and T cells into the IVD and amplify the inflammatory cascade. Herein, we demonstrated the presence

of *N*-Ac-PGP, a potent chemokine, in degenerative discs. The levels of *N*-Ac-PGP positively correlated with the Pfirrmann grade, suggesting that *N*-Ac-PGP may be involved in the process of IDD by promoting immune cell infiltration.

Activated neutrophils and polymorphonuclear cells from the peripheral blood of IBD patients have been shown to express the proteases that generate *N*-Ac-PGP [13, 33]. NP cells are widely accepted as a type of pro-inflammatory cell that releases proteases to promote disc matrix degradation [34–36]. NP cells were shown to express MMP8, MMP9, and PE *in vivo*. The levels of MMP8 and MMP9 were higher in NP tissues from the severe degeneration group than from the mild degeneration group. This suggests that, as IDD

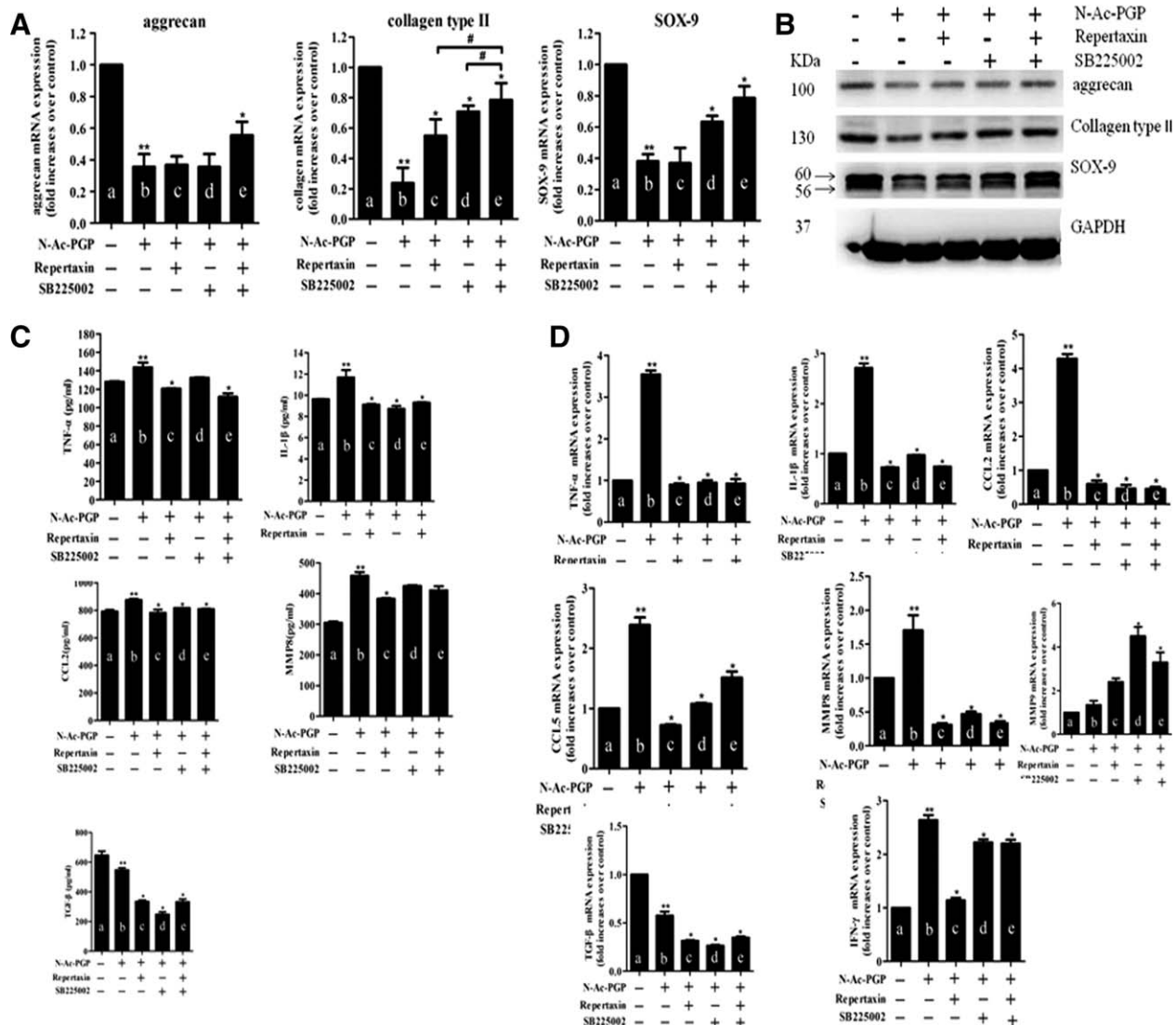


**Figure 5.** Effects of *N*-Ac-PGP on the differentiation of cartilage endplate stem cells (CECs). CECs were treated with or without *N*-Ac-PGP and the CXCR1 and CXCR2 antagonists. Total RNA was treated with DNase and processed for RT-PCR analysis to detect aggrecan, collagen type II, SOX-9, TNF- $\alpha$ , IL-1 $\beta$ , IFN- $\gamma$ , CCL-2, CCL-5, MMP8, MMP9, and TGF- $\beta$  expression (**A, D**). Total protein extracts were prepared and subjected to Western blot analysis of aggrecan, collagen type II, and SOX-9 (**B**). Conditioned media were harvested, and the levels of TNF- $\alpha$ , IL-1 $\beta$ , CCL-2, MMP8, and TGF- $\beta$  were quantitated by ELISA (**C**). \*\*,  $p < .05$  compared to a; \*,  $p < .05$  compared to b; #,  $p < .05$ . Abbreviation: *N*-Ac-PGP, *N*-acetylated proline-glycine-proline.

progresses, NP cells release more proteases to generate more *N*-Ac-PGP. Interestingly, we also found *in vitro* evidence to support this conclusion. The NP cell-conditioned media from the severe degeneration group contained more proteases and generated more *N*-Ac-PGP from collagen than from the mild degeneration group. The results indicate a negative role for NP cells in disc matrix degradation. This NP cell-mediated pathway of disc matrix degradation represents a new potential therapeutic target for IDD treatment.

*N*-Ac-PGP is a potent chemokine that signals through CXCR1/2 [11]. We verified that CECs constitutively express CXCR1 and CXCR2, and the expression of these receptors is upregulated by *N*-Ac-PGP treatment, suggesting that CXCR1 and CXCR2 are activated in response to *N*-Ac-PGP stimulation. *In vitro* chemotaxis assays indicated that *N*-Ac-PGP promotes the migration of CECs. Treatment with CXCR1 and CXCR2 antagonists individually or simultaneously inhibited this

migration. Furthermore, we found that *N*-Ac-PGP promoted the formation of F-actin and lamellipodia in CECs, and CXCR1/2 antagonists suppressed the *N*-Ac-PGP-mediated formation of F-actin and lamellipodia. F-actin cytoskeletal networks have been widely accepted as key regulators of cellular shape and force generation in cell migration [37]. These cytoskeletal networks are involved in the formation of lamellipodia, cell adhesion, and cellular shape changes. The formation of F-actin has been shown to be compatible with the increased migratory capability of tenocytes [38]. Herein, we also observed that the *N*-Ac-PGP-mediated formation of F-actin was compatible with the *N*-Ac-PGP-induced migration of CECs, suggesting that *N*-Ac-PGP rearranges F-actin cytoskeletal networks in CECs to increase their migratory capability. Intradiscal delivery of *N*-Ac-PGP in a rabbit lumbar disc model induced the migration of chondrocytes and spindle-shaped cells from the CEP into the notochord NP. The NP undergoes a chronological transition from a

notochordal to a fibrocartilaginous state that accompanies a change in cell type from a notochordal phenotype to a chondrocyte phenotype. Chondrocytes in fibrocartilaginous NP originate and migrate from the CEP into the NP in response to stimulation by soluble factors produced by notochordal cells [39, 40]. This natural NP transition is accelerated in the presence of CEP fracture [41]. In this study, intradiscal delivery of *N*-Ac-PGP into the rabbit notochord NP also accelerated the migration of chondrocytes from the CEP into the NP. CXCR1/2 antagonists suppressed this acceleration. Moreover, membrane-type I matrix metalloproteinase was expressed in these migrating chondrocytes, which was consistent with a previous study [41]. At a young age, notochord cells may degrade collagen to generate a small amount of *N*-Ac-PGP that is insufficient to trigger migration. However, over time or in pathological states such as CEP fracture, more *N*-Ac-PGP is generated to initiate the migration of chondrocytes and the NP transition. Interestingly, consistent with previous studies [39, 41], *N*-Ac-PGP also accelerated the migration of spindle-shaped cells in our study. These spindle-shaped cells, like MSCs, are believed to have the potential to differentiate into chondrocytes [39]. Moreover, we demonstrated the expression of Stro-1 and CD105 in the migratory spindle-shaped cells, indicating that these cells may be a type of MSC that resides in the rabbit CEP. Notably, we previously observed that the cells residing in human CEPs exhibited one cellular morphology indicative of round chondrocyte-like cells (Supporting Information Fig. S2A). However, there were two cell types in human CEPs, one was normal chondrocytes the other was chondrocyte-like cells that express MT-MMP1, Stro-1, and CD105 (Supporting Information Fig. S2B–S2D). The cells expressing MT-MMP1, Stro-1, and CD105 were regarded as human C ESCs which possess the migratory capacity [6, 20]. This suggests that all the cell types we have found in rabbit CEPs also exist in mature adult CEPs. Their morphology in vivo is different, perhaps because rabbits are skeletally immature. Thus, we boldly speculate that these spindle-shaped cells are rabbit C ESCs. Together, the in vitro and in vivo evidence suggest that *N*-Ac-PGP is a potent chemokine for disc cells.

The expression of aggrecan, collagen type II, and SOX-9 was downregulated by *N*-Ac-PGP, suggesting that C ESC differentiation toward an NP-like phenotype could be suppressed by certain mediators in the microenvironment of degenerative discs, although C ESCs migrate into the NP. As a result, C ESCs cannot enhance matrix synthesis and increase the number of functional cells in the IVD, suggesting a limited role for C ESCs in the structural and functional maintenance of the IVD. Moreover, C ESCs responded to *N*-Ac-PGP by increasing cytokine production. Consistent with the known effects of TLR activation on the immune plasticity of MSCs [8], in response to *N*-Ac-PGP, C ESCs acquired a pro-inflammatory phenotype characterized by decreased TGF- $\beta$  production and increased production of TNF- $\alpha$ , IL-1 $\beta$ , IFN- $\gamma$ , CCL2, CCL5, and MMP8. These alterations in protein expression, with the exception of TGF- $\beta$ , were suppressed by CXCR1/2 antagonists, suggesting that *N*-Ac-PGP binding to CXCR1/2 triggers an inflammatory cascade in C ESCs. Furthermore, *N*-Ac-PGP probably binds to other types of receptors to regulate the expression of TGF- $\beta$ . C ESCs possess immune plasticity that is regulated by *N*-Ac-PGP and its corresponding receptors. The results support the hypothesis that disc-derived cells initiate or amplify inflammatory signaling in the IVD.

The study of *N*-Ac-PGP-mediated inflammatory signaling is clinically relevant in IDD because endogenous *N*-Ac-PGP generated during IDD progression has the potential to activate C ESCs. C ESCs respond to *N*-Ac-PGP by migrating from the CEP into the NP and by differentiating toward a pro-inflammatory phenotype that elevates cytokine levels in the microenvironment of degenerative discs. IDD is associated with chronically increased levels of numerous pro-inflammatory cytokines that mediate matrix degradation, immune cell infiltration, and cell senescence in the IVD [9, 14, 25]. Pro-inflammatory C ESCs promote the progression of IDD, rather than suppressing it. The suppression of this pro-inflammatory differentiation relieves the inflammatory signaling in degenerative discs and contributes to their repair and regeneration. However, the immune plasticity of C ESCs is not fully understood and should be investigated in future studies.

There are limitations to our findings. One is that we used in vitro cultured human C ESCs to assess the effects of *N*-Ac-PGP on the migration and differentiation of C ESCs. In vivo evidence will be required in our further studies. The other is that rabbit discs are skeletally immature. The biochemical and biophysical microenvironment in the rabbit disc are different from that in the human degenerative disc. Other skeletally mature animal models will be used to perform in vivo assays in the future.

## CONCLUSIONS

Both the proteases that generate *N*-Ac-PGP and *N*-Ac-PGP itself are present in degenerative IVDs. *N*-Ac-PGP promotes the migration of C ESCs from the CEP into the NP via CXCR1/2. However, the binding of *N*-Ac-PGP to CXCR1/2 induces the differentiation of C ESCs toward a pro-inflammatory phenotype rather than an NP-like phenotype. This response limits the positive effects and promotes the negative effects of C ESCs on IVD regeneration. Thus, a better understanding of how to promote the positive effects and suppress the negative effects of C ESCs in disc regeneration will contribute to the development of C ESC-based biological therapies for IDD.

## ACKNOWLEDGMENTS

We thank American Journal Experts for their editing service. This study was supported by the National Natural Science Foundation of China (No. 81271982, No. 81472076 and No. 81572186).

## AUTHOR CONTRIBUTIONS

C.F.: conception and design, collection and/or assembly of data, data analysis and interpretation, and manuscript writing; Y.Zhang: collection and/or assembly of data and provision of study material or patients; M.Y.: collection and/or assembly of data and data analysis and interpretation; B.H.: conception and design and final approval of manuscript; Y.Zhou: final approval of manuscript, conception and design, financial support, and administrative support.

## DISCLOSURE OF POTENTIAL CONFLICTS OF INTEREST

The authors indicate no potential conflicts of interest.

## REFERENCES

- 1 Luoma K, Riihimäki H, Luukkonen R et al. Low back pain in relation to lumbar disc degeneration. *Spine* 2000;25:487-492.
- 2 Takatalo J, Karppinen J, Niinimäki J et al. Does lumbar disc degeneration on magnetic resonance imaging associate with low back symptom severity in young Finnish adults? *Spine* 2011;36:2180-2189.
- 3 Risbud MV, Albert TJ, Guttapalli A et al. Differentiation of mesenchymal stem cells towards a nucleus pulposus-like phenotype in vitro: Implications for cell-based transplantation therapy. *Spine* 2004;29:2627-2632.
- 4 Stoyanov JV, Gantenbein-Ritter B, Bertolo A et al. Role of hypoxia and growth and differentiation factor-5 on differentiation of human mesenchymal stem cells towards intervertebral nucleus pulposus-like cells. *Eur Cells Mater* 2011;21:533-547.
- 5 Liu LT, Huang B, Li CQ et al. Characteristics of stem cells derived from the degenerated human intervertebral disc cartilage endplate. *PLoS One* 2011;6:e26285.
- 6 Huang B, Liu LT, Li CQ et al. Study to determine the presence of progenitor cells in the degenerated human cartilage endplates. *Eur Spine J* 2012;21:613-622.
- 7 Huang YC, Leung VY, Lu WW et al. The effects of microenvironment in mesenchymal stem cell-based regeneration of intervertebral disc. *Spine J* 2013;13:352-362.
- 8 Romieu-Mourez R, Francois M, Boivin MN et al. Cytokine modulation of TLR expression and activation in mesenchymal stromal cells leads to a proinflammatory phenotype. *J Immunol* 2009;182:7963-7973.
- 9 Risbud MV, Shapiro IM. Role of cytokines in intervertebral disc degeneration: Pain and disc content. *Nat Rev Rheumatol* 2014;10:44-56.
- 10 Gaggari A, Jackson PL, Noerager BD et al. A novel proteolytic cascade generates an extracellular matrix-derived chemoattractant in chronic neutrophilic inflammation. *J Immunol* 2008;180:5662-5669.
- 11 Weathington NM, van Houwelingen AH, Noerager BD et al. A novel peptide CXCR ligand derived from extracellular matrix degradation during airway inflammation. *Nat Med* 2006;12:317-323.
- 12 O'Reilly P, Jackson PL, Noerager B et al. N-alpha-PGP and PGP, potential biomarkers and therapeutic targets for COPD. *Respir Res* 2009;10:38.
- 13 Koelink PJ, Overbeek SA, Braber S et al. Collagen degradation and neutrophilic infiltration: A vicious circle in inflammatory bowel disease. *Gut* 2014;63:578-587.
- 14 Kepler CK, Ponnappan RK, Tannoury CA et al. The molecular basis of intervertebral disc degeneration. *Spine J* 2013;13:318-330.
- 15 Pfirrmann CW, Metzger A, Zanetti M et al. Magnetic resonance classification of lumbar intervertebral disc degeneration. *Spine* 2001;26:1873-1878.
- 16 Modic MT, Masaryk TJ, Ross JS et al. Imaging of degenerative disk disease. *Radiology* 1988;168:177-186.
- 17 Schiebler ML, Camerino VJ, Fallon MD et al. In vivo and ex vivo magnetic resonance imaging evaluation of early disc degeneration with histopathologic correlation. *Spine* 1991;16:635-640.
- 18 Terti M, Paajanen H, Laato M et al. Disc degeneration in magnetic resonance imaging. A comparative biochemical, histologic, and radiologic study in cadaver spines. *Spine* 1991;16:629-634.
- 19 Kim H, Lee JU, Moon SH et al. Zonal responsiveness of the human intervertebral disc to bone morphogenetic protein-2. *Spine* 2009;34:1834-1838.
- 20 Xiong CJ, Huang B, Zhou Y et al. Macrophage migration inhibitory factor inhibits the migration of cartilage end plate-derived stem cells by reacting with CD74. *PLoS One* 2012;7:e43984.
- 21 Shibata A, Morioka I, Ashi C et al. Identification of N-acetyl Proline-Glycine-Proline (acPGP) in human serum of adults and newborns by liquid chromatography-tandem mass spectrometry. *Clin Chim Acta* 2009;402:124-128.
- 22 Hiyama A, Sakai D, Risbud MV et al. Enhancement of intervertebral disc cell senescence by WNT/beta-catenin signaling-induced matrix metalloproteinase expression. *Arthritis Rheum* 2010;62:3036-3047.
- 23 Le Maitre CL, Freemont AJ, Hoyland JA. The role of interleukin-1 in the pathogenesis of human intervertebral disc degeneration. *Arthritis Res Ther* 2005;7:R732-745.
- 24 Le Maitre CL, Hoyland JA, Freemont AJ. Catabolic cytokine expression in degenerate and herniated human intervertebral discs: IL-1beta and TNFalpha expression profile. *Arthritis Res Ther* 2007;9:R77.
- 25 Shamji MF, Setton LA, Jarvis W et al. Proinflammatory cytokine expression profile in degenerated and herniated human intervertebral disc tissues. *Arthritis Rheum* 2010;62:1974-1982.
- 26 Kawaguchi S, Yamashita T, Katahira G et al. Chemokine profile of herniated intervertebral discs infiltrated with monocytes and macrophages. *Spine* 2002;27:1511-1516.
- 27 Kepler CK, Markova DZ, Dibra F et al. Expression and relationship of proinflammatory chemokine RANTES/CCL5 and cytokine IL-1beta in painful human intervertebral discs. *Spine* 2013;38:873-880.
- 28 Gabr MA, Jing L, Helbling AR et al. Interleukin-17 synergizes with IFN-gamma or TNFalpha to promote inflammatory mediator release and intercellular adhesion molecule-1 (ICAM-1) expression in human intervertebral disc cells. *J Orthop Res* 2011;29:1-7.
- 29 Walsh AJ, Bradford DS, Lotz JC. In vivo growth factor treatment of degenerated intervertebral discs. *Spine* 2004;29:156-163.
- 30 Rowe SM, Jackson PL, Liu G et al. Potential role of high-mobility group box 1 in cystic fibrosis airway disease. *Am J Respir Crit Care Med* 2008;178:822-831.
- 31 Wang J, Tian Y, Phillips KL et al. Tumor necrosis factor alpha- and interleukin-1beta-dependent induction of CCL3 expression by nucleus pulposus cells promotes macrophage migration through CCR1. *Arthritis Rheum* 2013;65:832-842.
- 32 Takada T, Nishida K, Maeno K et al. Intervertebral disc and macrophage interaction induces mechanical hyperalgesia and cytokine production in a herniated disc model in rats. *Arthritis Rheum* 2012;64:2601-2610.
- 33 O'Reilly PJ, Hardison MT, Jackson PL et al. Neutrophils contain prolyl endopeptidase and generate the chemotactic peptide, PGP, from collagen. *J Neuroimmunol* 2009;217:51-54.
- 34 Rand N, Reichert F, Floman Y et al. Murine nucleus pulposus-derived cells secrete interleukins-1-beta, -6, and -10 and granulocyte-macrophage colony-stimulating factor in cell culture. *Spine* 1997;22:2598-2601; discussion 2602.
- 35 Kepler CK, Markova DZ, Hilibrand AS et al. Substance P stimulates production of inflammatory cytokines in human disc cells. *Spine* 2013;38:E1291-1299.
- 36 Yamamoto J, Maeno K, Takada T et al. Fas ligand plays an important role for the production of pro-inflammatory cytokines in intervertebral disc nucleus pulposus cells. *J Orthop Res* 2013;31:608-615.
- 37 Stricker J, Falzone T, Gardel ML. Mechanics of the F-actin cytoskeleton. *J Biomech* 2010;43:9-14.
- 38 Chang CH, Tsai WC, Lin MS et al. The promoting effect of pentadecapeptide BPC 157 on tendon healing involves tendon outgrowth, cell survival, and cell migration. *J Appl Physiol* 2011;110:774-780.
- 39 Kim KW, Lim TH, Kim JG et al. The origin of chondrocytes in the nucleus pulposus and histologic findings associated with the transition of a notochordal nucleus pulposus to a fibrocartilaginous nucleus pulposus in intact rabbit intervertebral discs. *Spine* 2003;28:982-990.
- 40 Kim KW, Ha KY, Lee JS et al. Notochordal cells stimulate migration of cartilage end plate chondrocytes of the intervertebral disc in vitro cell migration assays. *Spine J* 2009;9:323-329.
- 41 Kim KW, Ha KY, Park JB et al. Expressions of membrane-type I matrix metalloproteinase, Ki-67 protein, and type II collagen by chondrocytes migrating from cartilage endplate into nucleus pulposus in rat intervertebral discs: A cartilage endplate-fracture model using an intervertebral disc organ culture. *Spine* 2005;30:1373-1378.



See [www.StemCells.com](http://www.StemCells.com) for supporting information available online.